2007-01-2355

Application of the Modal Compliance Technique to a Vehicle Body in White

David Griffiths, Ph.D
Edward R. Green, Ph.D.
Roush Industries, Inc.

Kuang-Jen Liu, Ph.D.
DaimlerChrysler Corporation

ABSTRACT

This paper describes the application of the modal compliance method to a complex structure such as a vehicle body in white, and the extension of the method from normal modes to the complex modes of a complete vehicle. In addition to the usual bending and torsion calculations, the paper also describes the application of the method to less usual tests such as second torsion, match-boxing and breathing. We also show how the method can be used to investigate the distribution of compliance throughout the structure.

INTRODUCTION

The NVH characteristics of a vehicle depend strongly on its vibration modes. These in turn depend on the mass and stiffness distribution of the vehicle system, particularly that of the body. While the mass distribution is easily calculated, the stiffness distribution is not easy to calculate or measure. On the other hand, it is relatively easy to experimentally determine the vibration modes of vehicle bodies. Such tests are simplest when the body is removed from the rest of the vehicle system before testing, and the free-free modes are measured.

In principle the stiffness distribution of the body can be found from the modes using a method called matrix inversion. In practice this is very difficult. An alternate approach is to use the modal data to simulate static determinate tests which measure the compliance (i.e. reciprocal of stiffness) of the structure for a set of known loads. The use of this method to analyze simple lightly damped systems, such as frames, has been described in previous papers (1, 2). Here we describe its extension to more complex systems with greater amounts of damping.

One of the big advantages of modal testing is that a single modal test provides data which can be analyzed in many ways. The most obvious example is that a single modal test can provide estimates of bending and torsional stiffness, whereas two completely different static tests are required to find these results. Not only this, but the dynamic data can be used to find a whole set of useful numbers, such as second torsion compliance, front torsion compliance and match-boxing compliance. Static test determination of these compliances would require a separate static test with different fixtures for each type of compliance.

The previous papers (1, 2) describe a method which assumed normal modes. In practice we often encounter modes which are complex. Consequently the method has been extended to complex modes. This extension was first applied to the “almost” normal modes of a lightly damped BIP (body in prime).

THEORY

In paper (1) we showed that for a static determinate test involving only forces and translational displacements, all the forces (F_n) can be written in terms of a single generalized force F and a set of coefficients (χ_n) that depend only on the geometry and the scaling of the generalized force:

$$F_n = \chi_n F \qquad \sum_n \chi_n = 0 \qquad (1)$$

Tests involving moments and rotations can be analyzed in a similar fashion.

The static compliance (C) is calculated from the displacements (d_n) at the load and support points via:

$$C = \frac{\sum_n \chi_n d_n}{F} = \frac{D}{F} \qquad (2)$$

If the structure can be represented by real normal modes then each mode gives a contribution to the compliance, (*c)*:

$$c = \frac{\Sigma_p \Sigma_q \chi_p \chi_q \Psi_p \Psi_q}{m(2\pi f_r)^2} = \frac{(\Sigma_p \chi_p \Psi_p)^2}{m(2\pi f_r)^2} \qquad (3)$$

where:

Ψ_i = mode shapes at load and support points

m = modal mass

f_r = Resonant frequency

The total compliance is the sum of the compliances due to the individual modes. The sum of the contributions of all the modes may also be found by constructing a "compliance" transfer function and extrapolating it to zero Hz. The compliance function has the form:

$$\frac{D}{F} = \Sigma_p \Sigma_q \chi_p \chi_q \frac{d_p}{F_q} = -\frac{1}{(2\pi f)^2} \Sigma_p \Sigma_q \chi_p \chi_q \frac{a_p}{F_q} \qquad (4)$$

In the event the modes are complex it can be shown (see appendix) that the modal contribution is:

$$c = \frac{1}{(2\pi f_r)^2 m} \left[A^2 - B^2 + \frac{2\zeta}{\sqrt{1-\zeta^2}} AB \right] \qquad (5)$$

where:

$$A = \sum_p \chi_p \, \mathrm{Re}(\psi_p) \qquad (6)$$

$$B = \sum_p \chi_p \, \mathrm{Im}(\psi_p) \qquad (7)$$

In the case of real normal modes the equations (5), (6) and (7) reduce to equation (3) – but we should note that in practice real normal modes are often taken to be purely imaginary.

The total compliance is the sum of all the modal compliances:

$$C = \sum_{r=1}^{r=\infty} c_r \qquad (8)$$

This series should converge quickly because of the f^2 factor in the denominator of the expression for *c*. However, since one always sums over a finite set of modes one expects the dynamic calculation of compliance to be slightly less than the static result.

BIP CORRELATION STUDY

A vehicle body-in-prime (BIP: sheet metal without glass or closures) was used to validate the theory for a complex structure. This was done by comparing static and dynamic tests. The theory was also used to extend the compliance method to tests where static procedures would be difficult, for example match-boxing or second torsion.

TORSIONAL COMPLIANCE

Static Test Theory

Torsional tests involve applying equal and opposite torques, Γ and $-\Gamma$, at various locations along the structure, for example at the front and rear, and then measuring the net angular deflection Ω between the load points. Figure 1 shows the basic geometry of such a test.

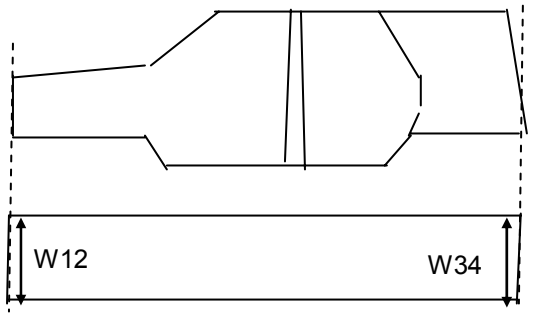

Figure 1: Torsion Test Geometry

Supposing that the applied forces F_p and deflections d_p are vertical at points 1, 2, 3 and 4, then we can define the forces and deflections via:

$$F_p = \chi_p \Gamma \qquad \Omega = \sum_p \chi_p d_p \qquad (9)$$

The torsional compliance is then:

$$C = \frac{\Omega}{\Gamma} = \frac{\sum_p \chi_p d_p}{\Gamma} \qquad (10)$$

The values of the $\chi's$ are determined from:

$$\chi_1 = \frac{1}{W_{12}} = -\chi_2 \qquad \chi_3 = -\frac{1}{W_{34}} = -\chi_4 \qquad (11)$$

Strictly speaking this type of test is "less-than-static-determinate" in the sense that the specification of static test forces allows an overall rigid body motion. However the method of calculating compliance removes rigid body motion, and we have static results which can be compared exactly to free-free modal results.

Static Results

The body structure was supported and loaded at the ends of the front and rear rails. Various loads were applied and the structure was found to be quite linear for torques up to 500 N-m.

End-to-end torsional compliance: 1.55 x10^{-6} rad/N-m

Dynamic Results & Correlation

The complex mode calculation for end to end torsion gave 1.47 x10^{-6} rad/N-m. This was approximately 95% of the static result, so the results of the dynamic method agreed well the static results.

The compliance was spread among a number of modes as shown in Table 1. Note that modes with negligible contribution are not shown.

Table 1: Modal Contributions to Overall Torsional Compliance

Mode Freq. (Hz)	Compliance per Mode Rad/N-m	Cumulative Compliance	% Total
31.95	4.44E-07	4.44E-07	30.3
37.01	4.27E-07	8.71E-07	59.4
38.53	1.49E-07	1.02E-06	69.5
46.26	1.09E-07	1.13E-06	77.0
64.35	9.02E-08	1.22E-06	83.1
66.93	3.28E-08	1.25E-06	85.3
71.72	2.11E-08	1.27E-06	86.8
73.61	1.85E-08	1.29E-06	88.0
78.71	5.82E-08	1.35E-06	92.0
100.15	3.61E-08	1.39E-06	94.5
103.27	3.49E-08	1.42E-06	96.9

Most of the compliance (~60%) is contributed by the two modes at 31.95 Hz and 37.01 Hz, and a further 20% of the compliance is contributed by the modes at 38.5, 46.3 and 64.4 Hz. Some modes gave negative contributions with very small magnitudes, an effect that was attributed to curve-fitting issues.

Torsional Stiffness Distribution

When analyzing torsional compliance it is tempting to suppose that the body structure can be treated as torsional springs in series. This is certainly a convenient starting point. However, two points need to be born in mind: (a) the structure of the body is sufficiently non-uniform that the concept of springs in series can only be a rough approximation (b) as the analyzed sub-divisions are made smaller the fractional errors of measurement become larger.

The first step in analyzing the distribution of torsional stiffness was to consider the body as a front and rear section: front of the body to the B-pillars and B-Pillars to the rear. The torsional compliances were then found for these sections and their sum compared to the complete vehicle compliance. Figure 2 summarizes the results.

It is evident that the rear section is stiffer (less compliant) than the front, and that the sum of the front and rear compliance is close to the overall compliance. Some negative contributions at high frequencies indicate curve fitting problems.

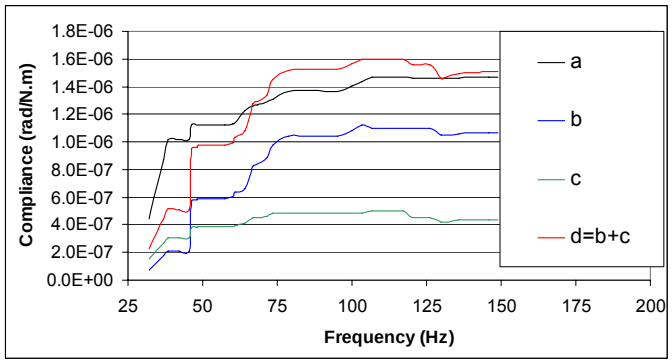

Figure 2: Cumulative Torsional Compliance
(a) End to End (b) Front to B-Pillar
(c) B-Pillar to Rear (d) Sum b+c

The use of modal data makes it easy to subdivide the body even further, for example into (a) front to dash (b) dash to center (c) center to C-Pillar (d) C-pillar to rear. The results of this analysis are shown in Table 2.

Table 2: Compliance of Body-Subdivisions (rad/N-m)

	Compliance Rad/N-m	**Compliance as % of End-End**
End-End	1.4E-06	100
Front-dash	5.5E-07	38.5
dash-center	1.5E-07	10.4
center-C-Pillar	2.2E-07	15.5
C-Pillar-Rear	1.3E-07	8.8
Sum	1.1E-06	73.1

It can be seen that the compliance of the sub-divisions almost adds to the total, supporting the idea that for torsional purposes the body can be represented by springs in series, at least as far as the 4-section breakdown analyzed here.

2nd Torsion Compliance

More insight into the compliance distribution can be obtained by investigating 2nd torsion, i.e. torsion exhibited by modes where the front and rear rotate together out of phase with the center.

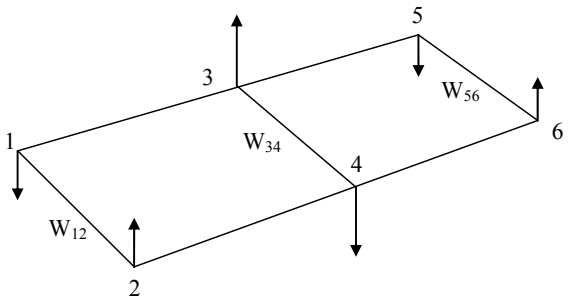

Figure 3: 2nd Torsion Geometry

The equivalent static test would involve applying a torque to the center of the vehicle (B-Pillar area) while restraining the ends, then measuring angular twist versus applied torque. The choice of restraining force is somewhat arbitrary, here we choose the front and rear restraining torques to be equal.

The applied forces are then defined in the usual way:

$$F_p = \chi_p \Gamma \qquad \chi_3 = \frac{1}{W_{34}} = -\chi_4$$

$$\chi_1 = \frac{-.5}{W_{12}} = -\chi_2 \qquad \chi_5 = \frac{-.5}{W_{56}} = -\chi_4 \tag{12}$$

$$C = \frac{\sum_p \chi_p d_p}{\Gamma} \tag{13}$$

For the vehicle under consideration the modal data gave a compliance value of 4.6 x 10^{-7} rad/N-m, and the main modal contributions were as shown in Table 3 below:

Table 3: 2nd Torsion Compliance by Mode

Mode Frequency	% Contribution to Total Compliance
46.3	41.7
66.9	19.5
73.6	11.1

BENDING COMPLIANCE

Static Test Theory

Bending tests involve applying equal forces F/2 at the center of the structure (points 3 and 4), supporting the structure at the ends (points 1, 2, 5 and 6), and measuring the average deflection at the center. The forces and compliance are defined in the usual way. The values of the $\chi's$ are determined from the geometry and load definition:

$$\chi_1 = -\frac{L_{35}}{2L_{15}} = \chi_2 \qquad \chi_3 = \frac{1}{2} = \chi_4$$

$$\chi_5 = -\frac{L_{13}}{2L_{15}} = \chi_6 \tag{14}$$

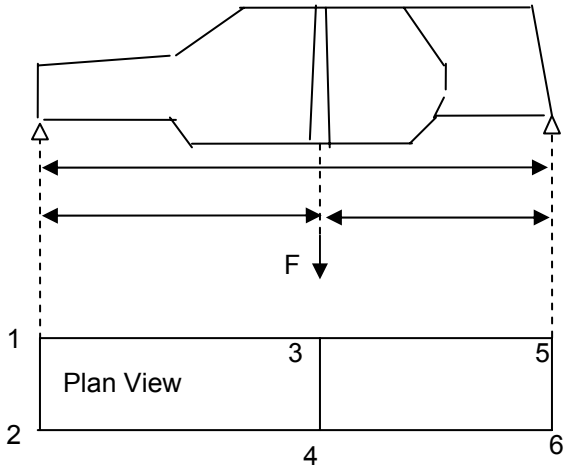

Figure 4: Geometry of Test Set-Up for Overall Bending

Static Test Results

The body structure was supported at its front & rear rails and loaded near the center. The structure was found to be quite linear. The compliance was computed from the deflections with a load of 800 N (400 N on either side). The results are summarized in Table 4.

Table 4: Static Bending Compliance Test Measurement & Calculation

Point #	d_i	χ_i	$\chi_i d_i / F$ (m/N)
1	6.35E-05	-0.2540	-2.0147E-08
2	8.13E-05	-0.2540	-2.5788E-08
3	5.84E-05	-0.2460	-1.7948E-08
4	2.11E-04	-0.2460	-6.4771E-08
5	3.97E-04	0.5000	2.4766E-07
6	3.07E-04	0.5000	1.9156E-07
	Total Compliance		3.1056E-07

The deflection at support #4 was 4 times the deflection at support 3, indicating a lack of symmetry in the set-up, and this lack of symmetry could be expected to "contaminate" the bending results to some extent.

Dynamic Test Results

The total end to end compliance determined from the modes was 2.45E x 10^{-7} m/N or approximately 80% of the static result. This agreed reasonably well with the static results considering the problem at support #4.

Table 5: Modal Contributions to Overall Bending Compliance

Freq. Hz	Compliance m/N	%Total
42.2	3.72E-08	15.2
45.5	1.09E-07	44.4
48.2	5.44E-08	22.2
48.5	3.86E-08	15.7
60.2	1.68E-09	0.7
60.8	3.03E-09	1.2
64.4	4.80E-09	2.0
73.6	2.55E-09	1.0
106.8	-6.85E-09	-2.8
120.5	-1.23E-09	-0.5
Sum	2.43E-07	99.1

The contribution of the modes is shown in Table 5 (only the more important modes are shown). Essentially all the compliance was provided by 4 modes in the range 42 – 49 Hz, other modes giving negligible contributions. Some modes gave small negative contributions, probably due to curve fitting problems.

Distribution of Bending Compliance

The modal compliance method makes it relatively easy to examine the distribution of bending compliance in a structure. As an example, Figure 5 shows one possible way to analyze front and rear bending.

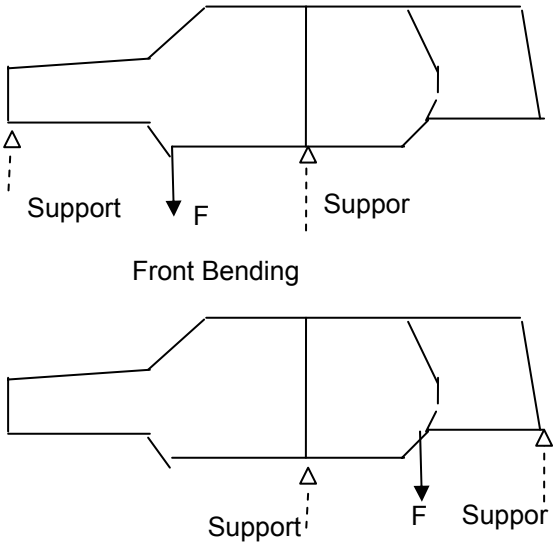

Figure 5: Geometry for Front & Rear Bending

Note that if the structure was a uniform beam then the bending compliance would be proportional to the cube of the length of the section analyzed. For this reason we compare both the compliance and the compliance scaled by the cube of the section length, as shown in Table 6 below.

Table 6: Front & Rear Bending Compliance vs. Overall Compliance

	Compliance (m/N)	Compliance *(L/Li)^3	Scaled/Overall
Overall	2.45 E-07	2.45 E-07	100%
Front	1.52 E-08	1.28 E-07	52%
Rear	5.35 E-08	4.08 E-07	166%
	Sum F+R (Weighted)	2.68 E-07	109%

Match-boxing

Theory

Match-boxing refers to the sort of deformation often seen in rectangular sections (“match-boxes”) when a vertical or horizontal shear load is applied. The top moves laterally relative to the bottom in a shearing motion (see Figure 6), one diagonal is compressed (1-3) while the other is stretched (2-4).

This type of motion often occurs in vehicle body torsional modes. Given that the structure has a plane of symmetry, the match-boxing is anti-symmetric, that is, the left-right symmetric points have the same lateral motion but the opposite vertical motion. As a result points 1 and 3 move towards and then away from each other, and move out of phase with points 2 and 4. Note that usually the widths W_{12} and W_{34} are nearly equal.

We define match boxing forces so as to exaggerate the effect (see Figure 6).

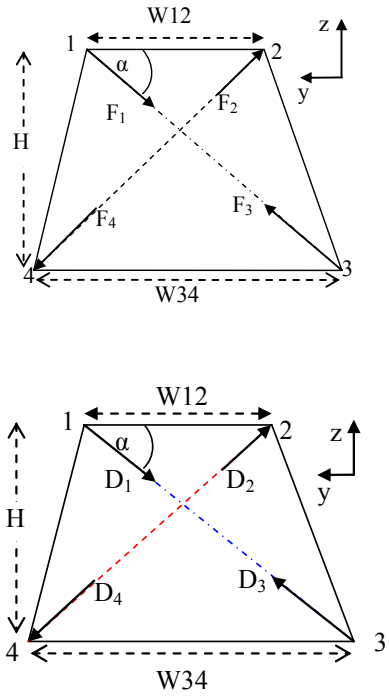

Figure 6: Match-boxing Motion & Forces

If we write the forces in terms a generalized force we can then define the match-boxing compliance in the usual form:

$$C = \frac{D}{F} = \frac{\sum_p \chi_p d_p}{F} \qquad (15)$$

Here the index p covers both location and direction (p=1y,1z,2y,2z,.....). and the value of each χ is determined from the geometry (see appendix).

Modal Results

The main contributing modes are shown in Table 7.

Table 7: Distribution of Match-Boxing Compliance

Frequency	Compliance (m/N)	% Total
31.90	6.41E-07	38.5
37.00	5.25E-07	31.6
46.30	9.59E-08	5.8
100.15	6.29E-08	3.8
135.78	7.82E-08	4.7
Sum	1.40E-06	84.3

The match-boxing compliance in the B-pillar region was determined from the modal data and found to be 1.4 x 10^{-6} m/N. The static match-boxing compliance was measured as 1.19e-9 m/N. The difference between the modal and static result was 18%.

The distribution of compliance among the modes is similar to that of torsion, with the major exception that there is a mode at 38.5 Hz which contributes 10% to torsional compliance but essentially zero to match boxing compliance.

Breathing Compliance

We use the term breathing to apply to a symmetrical in-out motion, for example the center roof and center floor moving vertically in opposite directions as illustrated in Figure 7.

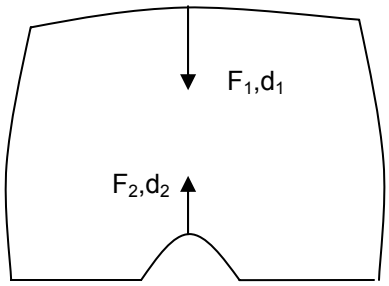

Vertical Breathing

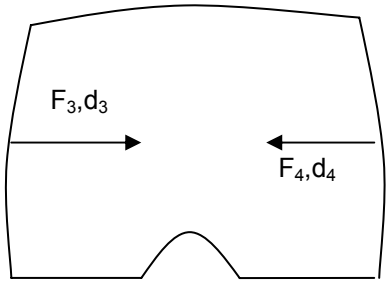

Lateral Breathing

Figure 7: Geometry of Breathing Compliance

The vertical and lateral breathing compliance are given by:

$$C_V = \frac{d_1 - d_2}{F_V} \qquad C_L = \frac{d_3 - d_4}{F_L} \qquad (16)$$

where:

$$F_1 = F_V = -F_2$$
$$F_3 = F_L = -F_4 \qquad (17)$$

These formulas make it relatively easy to find the vertical & lateral compliance. At the B-pillars the compliances were found to be:

C_V= 2.1 x10^{-6} N/m C_L=1.26 x10^{-7} N/m

The compliance distribution among the modes is shown in Table 8.

Table 8: Distribution of Breathing Compliance

	Mode Contribution %	
Modal Frequency	**Vertical Breathing**	**Horizontal Breathing**
42.2	29.7	46.2
48.2	27.5	14.5
48.5	10.2	7.7
64.4		4.4
86.6		3.
95.1		10.7
100.2		1.74
110.2		1.46
120.5	29.8	
Cumulative %	97	90

FULL VEHICLE TORSION

A full vehicle (complete body, engine, suspension, etc) was used to check the ability of the method to detect torsional modes, and the reasonableness of the results. The vehicle was of the same type from which the BIP was extracted, and the vehicle was excited at the corners near the ends of the rails. The extracted modes, which in some cases were quite complex, were used to calculate the torsional compliance. The results were then compared with (a) subjective descriptions of the modes and (b) the BIP compliance.

Table 9: Full Vehicle Compliance by Mode

Mode	Compliance		Description
Freq. Hz	%	Rad/N-m	
20.4	1.5	7.3 x10^{-9}	Various Local Motions
21.8	2.1	10.4 x10^{-9}	Various Local Motions
22.7	41.	200 x10^{-9}	Body Torsion
27	2.1	10.1 x10^{-9}	Body & Exhaust Bending
28.2	4.1	20.2 x10^{-9}	Steering Col. vertical
30.3	3.3	16.2 x10^{-9}	Minor Front-End Torsion
31	18	86 x10^{-9}	Front End Torsion

Table 9 shows the calculated compliance by mode for modes contributing more than 1% of the total compliance, and modes which subjectively exhibited torsion. The subjective description is given for comparison. It can be seen that the modal compliance method is very effective at identifying the 22.7 and 31 hz torsional modes.

The total calculated compliance was 4.9x10^{-7} rad/N-m. This is to be compared with the BIP compliance, 14.x 10^{-7} rad/N-m. Adding fixed glass to the BIP can be expected to reduce the compliance by a factor of ~ ½, and addition of closures (doors, hatchback, etc.) will also reduce the compliance. Consequently we conclude that the full vehicle results are consistent with the BIP results.

CONCLUSIONS

The studies described in this paper show that when the modal compliance method is applied to complex but lightly damped structures such as a BIP:

(a) It provides accurate estimates of overall torsion and bending compliance as measured in static determinate tests.

(b) It can be used to estimate the distribution of torsional and bending compliance for the structure.

(c) It can be extended to "unusual" analysis such as 2nd torsion, match-boxing and breathing compliance.

(d) It can be applied to complex modes.

In addition, when the method is applied to complex and heavily damped systems such as complete vehicles, it can identify major body torsional modes and provide a reasonable estimate of the body torsional compliance.

REFERENCES

1. D. Griffiths, A. Aubert, E. Green, J. Ding, *A Technique for Relating Vehicle Structural Modes to Stiffness as Determined in Static Determinate Tests*, SAE 2003-01-1716

2. D. Griffiths and W. S. Stevenson, *Dynamic Determination of Local Bracket Compliance*, IMAC XXII, 2004, 145

3. R. Potter & M. Richardson, *Mass, Stiffness & Damping Matrices from Measured Modal Parameters*, ISA-630, 74-630

APPENDIX

Appendix: Derivation of Formulas

Transfer Functions & Complex Modes

In the standard modal theory each mode is parameterized by:

M = modal mass
K = modal stiffness
ψ_p =mode shape at degree of freedom p
ζ = viscous damping factor (fraction of critical damping)

$$\omega_r = \sqrt{(K/M)}$$
$$\hat{\omega}_r = \omega_r \sqrt{1-\zeta^2} \qquad (18)$$

The contribution of each mode to the compliance function is given by (3):

$$\frac{d_p(s)}{F_q(s)} = \left[\frac{\psi_p \psi_q}{a_r (s - s_r)} + \frac{\overline{\psi}_p \overline{\psi}_q}{\overline{a}_r (s - \overline{s}_r)} \right] \qquad (19)$$

Here the "bar" indicates the complex conjugate, and *s* is the Laplace variable:

$$s = i\omega = i(2\pi f) \qquad i = \sqrt{-1}$$
$$s_r = i\omega_+ = -\zeta\omega_r + i\tilde{\omega}_r \qquad (20)$$

The factor a_r is usually expressed in terms of a real modal mass or stiffness, for example:

$$a_r = 2i\tilde{\omega}_r M = 2\tilde{s}_r M \qquad (21)$$

Based on this the value of the compliance function at ω=0 is:

$$\frac{d_p(0)}{F_q(0)} = -\left[\frac{\psi_p \psi_q}{a_r s_r} + \frac{\overline{\psi}_p \overline{\psi}_q}{\overline{a}_r \overline{s}_r} \right] = -2\,\mathrm{Re}\left[\frac{\psi_p \psi_q}{a_r s_r} \right] \qquad (22)$$

Expressing a_r in terms of the modal mass (assumed real), and with a little algebra we find:

$$\frac{d_p(0)}{F_q(0)} = \frac{1}{\omega_r^2 M} \left[\mathrm{Re}\{\psi_p \psi_q) + \frac{\zeta}{\sqrt{1-\zeta^2}} \mathrm{Im}\{\psi_p \psi_q\} \right] \qquad (23)$$

Note that software packages often give "acceleration" mode shapes, and to get the appropriate "displacement" mode shapes one must divide each shape by $i\omega_r$. Also, we could extend this formula to complex modal mass, but this is not very useful since the modal mass can always be made real, and all the complexity can be factored into the mode shapes.

Compliance Calculation

The generalized static determinate compliance is obtained from the transfer functions via:

$$c = \sum_{p,q} \chi_p \chi_q \frac{d_p(0)}{F_q(0)} \qquad (24)$$

Based on this the contribution of an individual mode, assuming the modal mass *M* is real:

$$c = \frac{1}{\omega_r^2 M} \sum_{p,q} \chi_p \chi_q \left[\mathrm{Re}\{\psi_p \psi_q) + \frac{\zeta}{\sqrt{1-\zeta^2}} \mathrm{Im}\{\psi_p \psi_q\} \right] \qquad (25)$$

Given that the χ'*s* are real, this expression can be written in a more convenient form for computation:

$$c = \frac{1}{(2\pi f)^2 M} \left[A^2 - B^2 + \frac{2\zeta}{\sqrt{1-\zeta^2}} AB \right] \qquad (26)$$

where:

$$A = \sum_p \chi_p \,\mathrm{Re}(\psi_p)$$
$$B = \sum_p \chi_p \,\mathrm{Im}(\psi_p) \qquad (27)$$

Match-boxing Compliance Calculations

General Approach

As usual we wish to define the match-boxing compliance *C* in terms of a static determinate test defined by a generalized force *F* and a displacement *D*. In this case some forces and displacements are in the y direction, and some in the *z*-direction. For this reason we modify the usual formulas so that:

$$F_{py} = \chi_{py} F \qquad F_{pz} = \chi_{pz} F$$
$$D = \sum_p \{\chi_{py} d_{py} + \chi_{pz} d_{pz}\} \qquad (28)$$

To make equations more compact we will in practice give each degree of freedom a single index.

Forces & Constraints

The appropriate load geometry is shown in Figure 8.

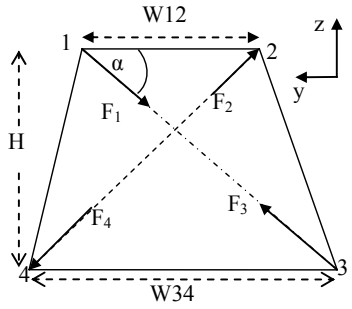

Figure 8: Loads & Constraints for Match-Boxing

For convenience we will define the generalized force *F* via:

$$\vec{F}_1 = \vec{F} = -\vec{F}_3 \qquad (29)$$

Here the horizontal arrows are used to denote vector quantities. F_2 has the same *y* component as F_1, but the sign of the *z* component is reversed:

$$F_{2y} = F_{1y} \qquad F_{2z} = -F_{1z} \qquad (30)$$

F_4 is the negative of F_2

$$\vec{F}_4 = -\vec{F}_2 \qquad (31)$$

Working in terms of Cartesian coordinates we have (|*F*|=magnitude of generalized force):

$$F_{1y} = -|F|\cos(\alpha) = F_{2y} = -F_{3y} = -F_{4y} \qquad (32)$$

$$F_{1z} = -F\sin(\alpha) = -F_{2z} = -F_{3z} = +F_{4z} \qquad (33)$$

The required χ's are now easily found. Representing the indices by a single index, *p* or *q*, we then have

$$F_p = \chi_p F \qquad (34)$$

Generalized Displacement

The deflection geometry is shown in Figure 9.

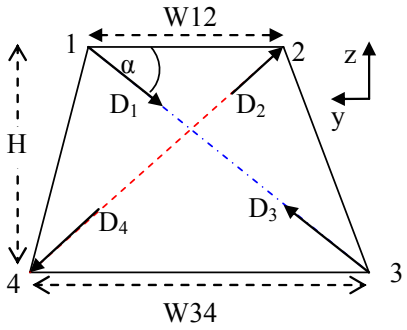

Figure 9: Match-Boxing Deflections

We will define the generalized match-boxing displacement as the sum of the 1-3 compression and the 2-4 expansion, with sign conventions as in the diagram:

$$D = \sum_p D_p \qquad (35)$$

If we denote the y and z displacements at point 1 as d_{1y} and d_{1z}, then the net match-boxing motion D_1 along the F_1 direction is :

$$\begin{aligned} D_1 &= -d_{1y}\cos(\alpha) - d_{1z}\sin(\alpha) \\ &= \chi_{1y} d_{1y} + \chi_{1z} d_{1z} \end{aligned} \qquad (36)$$

In general we can define the match-boxing displacements along the direction of all 4 forces in the same way, and the total displacement is given by:

$$D = D_1 + D_2 + D_3 + D_4 = \sum_p \chi_p d_p \qquad (37)$$